Study on the influence of the modelling strategy in the calculation of the worn profile of railway wheels

STUDY ON THE INFLUENCE OF THE MODELLING STRATEGY IN THE CALCULATION OF THE WORN PROFILE OF RAILWAY WHEELS

NICOLA BOSSO*, MATTEO MAGELLI† & NICOLÒ ZAMPIERI‡
Politecnico di Torino, Department of Mechanical and Aerospace Engineering, Italy

ABSTRACT
As changes in the wheel and rail profiles strongly affect vehicle dynamics, running stability and safety, maintenance operations such as wheel turning and rail grinding are necessary. The availability of numerical models for wear prediction can be a huge support to optimize the scheduling of such operations. Thanks to the computational power of modern computer architectures, allowing parallelization and co-simulation, the typical strategy is based on a dynamic module performing the vehicle dynamics simulation, usually developed in commercial multibody (MB) software packages, and on a wear module for the calculation of the worn material. The latter can be implemented in the same MB code or in a separate software, such as Matlab/Simulink, which exchanges data with the MB code. Wear modules rely on wear laws relating the amount of worn material to the normal load and sliding distance or to the energy dissipated at the contact interface. Both types of law can be applied locally, calculating the worn depth in each cell of the discretized contact patch from the contact pressures and sliding speeds, or globally, hence calculating the worn volume or mass starting from the global forces and creepages. In the latter case, the worn material is calculated on the whole contact patch rather than only on the slip zone, and a proper distribution is required to relate the worn depth to the worn volume. The present work aims to further investigate the differences between the two approaches in the computed worn profiles in a specific case study in terms of reference vehicle and track, carrying out the dynamic simulations through the Simpack MB code. The paper is intended to highlight the differences in both the numerical results and computational efforts, comparing the wear computed by a local model with the outputs of the Simpack wear module.
Keywords: wheel wear, worn profiles, wheel–rail tribology, wheel–rail contact, Archard wear law, dynamic simulation, multibody simulation.

1 INTRODUCTION

Uniform wear, i.e., the change in the wheel transversal profile shape due to wear, has a strong impact on the running behaviour of railway vehicles. To ensure safety, the wheel profiles undergo periodical maintenance so that the original profile shape can be restored thanks to machining operations. Such maintenance operations are typically scheduled at fixed travelled distances, but this strategy neither prevents possible premature failures of the wheel nor it ensures that turning is indeed necessary when performed. Therefore, modelling the wear of the wheel transversal profile is crucial to predict the damage of the wheels and to optimally schedule the maintenance interventions, with obvious economic benefits.

Currently, the typical strategy adopted to predict wear of wheel profiles is based on numerical tools that include a module for the vehicle-track dynamic simulation, usually implemented in a commercial multibody (MB) software package, and a module that computes the worn profile starting from the outputs of the dynamic simulation [1]. In the past, the wear module was implemented in the MB code used for the dynamic simulation in

* *ORCID: https://orcid.org/0000-0002-5433-6365*
† *ORCID: https://orcid.org/0000-0002-2962-7873*
‡ *ORCID: https://orcid.org/0000-0002-9197-1966*

WIT Transactions on The Built Environment, Vol 213, © 2022 WIT Press
www.witpress.com, ISSN 1743-3509 (on-line)
doi:10.2495/CR220061

the form of a user-written routine, while nowadays several wear computation tools rely on co-simulation approaches, with the wear module implemented in a different computational environment [2]. Moreover, all commercial MB codes are currently provided with add-ons for the calculation of the wheel worn profile. These built-in modules ensure a fast setting of the wear computation thanks to user-friendly graphical interfaces (GUIs). Commonly, wear is computed at discrete steps, so that the wheel profile is considered unchanged during a single dynamic simulation, but at the end of each step of the wear calculation the profile is updated and fed back to the dynamic simulation module. This strategy is far more accurate with respect to the simplified approaches adopted in the past, in which the wheel profile was updated at discrete steps without launching new dynamic simulations [3], [4].

The amount of worn material is computed as a function of the main contact patch quantities by means of wear laws obtained from experimental campaigns. Two main types of wear laws are available in the literature, namely laws that relate the worn material to the normal load acting on the contact patch and laws that relate wear to the dissipated energy. The most common wear law based on the normal load is the Archard law [5], [6], while examples of wear laws based on the dissipated energy include equations proposed by British Railway Centre (BRR) [7], University of Sheffield (USFD) [8], Krause and Poll [9] and Zobory [10].

Most of the above-mentioned wear laws can be applied either globally or locally. In the first case, the worn material is computed directly from the global forces and creepages acting at the contact patch, while with the second approach, the wear depth is computed in each cell of the contact patch grid. Clearly, the first approach ensures a faster computation, but it requires the development of a strategy to spread the worn material along the profile transversal coordinate. On the other hand, the second solution allows to directly compute the wear depth locally, but it demands a local contact module that performs the discretization of the contact patch to obtain the distribution of the tangential pressures and slip velocities.

In a recent paper, Peng et al. [11] suggested that a global application of the wear laws is not suitable when the wear computation focuses on irregular wear along the circumferential direction ("wheel polygonization"), due to the generation of sharp points in the wear depth distribution. Nonetheless, for what concerns uniform wear of the wheel profile, different works in the literature indicate that the global approach might be the best compromise solution in a trade-off between numerical accuracy and computational efficiency. Researchers from USFD and Alstom Ferroviaria found that that the wheel worn transversal profiles computed with local and global applications of the USFD law were in good agreement with each other, with a maximum error of 20% [12]. Nevertheless, the investigation was not extended to other wear laws, therefore there is still a lack of knowledge for what concerns different equations.

Furthermore, based on the authors' experience and industrial collaborations, there is still a big need to assess the validity of the wear computed by the built-in modules implemented in commercial MB codes. This aspect was not addressed by USFD and ALSTOM researchers, as both global and local approaches were implemented in a post-processing in-house Matlab routine. To gain further insights into the problem, Ignesti et al. [13] compared the results computed by the Simpack wear module, which adopts a global approach, with the outputs of a local wear model implemented in a user-written Matlab routine. The authors of the cited reference found a generally good agreement between the two models, with Simpack predicting slightly larger wear. However, the main drawback of this work is that while the Simpack global wear model used the Krause–Poll law, the local wear model relied on the USFD wear law. Therefore, the cited reference did not directly compare the implementation

of the same wear law in a global application of a MB code and in a local application in a user-written routine.

The present work aims at gaining a better understanding of the differences due to global and local applications of wear laws in the calculation of the wheel worn profile, adopting the Simpack wear module as the reference for the global calculation. The wear law considered in the present paper is the Archard wear law in the implementation of the Swedish Royal Institute of Technology (KTH). Such law is available in the Simpack wear module and it can be applied locally.

Often, when using local approaches, the dynamic simulation calculates the wheel–rail forces by means of fast heuristic methods [14]–[16], while the discretization of the contact patch is carried out only by the local contact model implemented in the wear module. Nonetheless, this approach can lead to inconsistent results as different algorithms for the computation of the tangential forces rely on different relations between forces and creepages, and correction factors should be introduced in the local contact model to improve accuracy [17], [18]. Therefore, in the present paper, the tangential forces are computed implementing the FASTSIM [19] algorithm in both the dynamic simulation and in the local wear model.

The paper is organised as follows. The next section describes the numerical model of the vehicle and track considered in the present work, also giving focus to the algorithms adopted to compute the worn profile with global and local approaches. Then, the results of the proposed numerical activity are shown and discussed, and finally a last section highlights the main conclusions and suggests possible future developments of the proposed activity.

2 NUMERICAL MODEL

2.1 Vehicle-track dynamic model

The vehicle considered in the present work is the diesel powered Aln 663 railcar, which is a vehicle running mainly on secondary lines. The railcar is equipped with a hydromechanical 5-gear manual transmission, and it reaches a maximum speed of 120 km/h. The vehicle includes two FIAT bogies, with primary and secondary suspensions realized with helical springs. For each bogie, the inner wheelset is powered, while the outer one is trailed.

The railcar model was developed in the Simpack MB software package, and it consists of one coach, two bolsters, two bogie frames, four wheelsets and eight axle-boxes. A sketch of the model structure is given in Fig. 1. Each axle-box features a single degree of freedom (d.o.f.), i.e., the relative rotation with respect to the corresponding wheelset, and it is connected to the bogie frame via two force elements. The first force element is a flexicoil spring, with axial and shear stiffnesses, while the second force element is used to simulate the rubber joint connecting the axle-box control arm to the bogie frame. The secondary suspension is simulated by introducing another set of flexicoil springs, that connect the bogie frame to the bolster. Each bolster is rigidly connected to the railcar coach via proper bushing elements, with large stiffness values along each direction except for the rotation along the vertical direction, which is free. Moreover, the secondary suspension incudes two lateral bumpstops that provide a reaction force when the lateral displacement between the bolster and the bogie frame exceeds a prescribed threshold value. Finally, two lateral and two vertical linear dampers are added between each bolster and bogie frame, as a part of the secondary suspension.

Since the scope of the present work is the comparison between the local and global approaches in the calculation of the worn wheel profile, the simulated track is a simplified

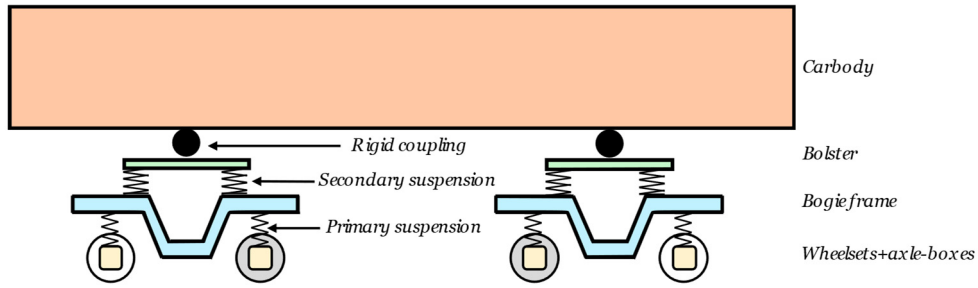

Figure 1: Sketch of the MB model architecture (powered wheelsets are coloured in grey).

track rather than a real track. The simplified track includes four different curves, with prescribed superelevation values, that are faced in both left and right-hand direction. All curves are separated by straight sections. Fig. 2 shows the curve radius along the track and the speed profile superimposed to the vehicle, while Table 1 presents the values of curve radius and superelevation for each curve. To directly compare the global and local approaches in wear computation, the track is modelled without irregularities and the rail profiles (UIC60) are considered as unworn along the whole reference track length. Please note that since curves are faced in both left and right-hand direction and that the wheel profiles (S1002) are considered as unchanged during the simulation, the wear of the left and right wheels belonging to the same wheelset is extremely similar. In the present work, wear is computed on the right wheel of the leading wheelset, which is a non-powered axle. The speed profile is followed by applying braking torques to the powered axles of the vehicle, thus simulating dynamic braking operations. The value of these torques is computed during the simulation taking into consideration the adhesion limit.

The determination of the wheel–rail contact points and the solution of the normal problem, i.e., the computation of the normal force and of the shape and size of the contact patch, is

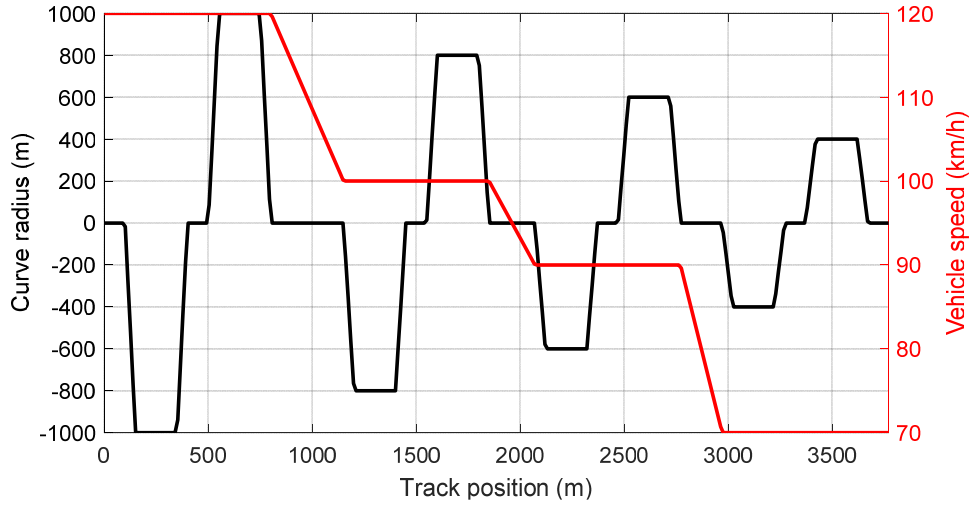

Figure 2: Speed profile and curve radius along the simulated track.

Table 1: Curves included in the simulated simplified track.

Curve radius (m)	Main curve parameters	
	Superelevation (mm)	Vehicle speed (km/h)
1000	150	120
800	150	100
600	160	90
400	160	70

carried out by means of Simpack built-in algorithms. The normal problem is solved using the equivalent elastic approach [20], which transforms the actual shape of the contact patch, obtained using the Kik–Piotrowski method [21], into an equivalent ellipse. The tangential problem, i.e., the calculation of the tangential forces, is solved using the FASTSIM algorithm by Kalker, directly available in Simpack. The profiles of wheels and rails are the standard S1002 and UIC60 profiles, respectively, and the friction coefficient is assumed constant and equal to 0.4, so that falling friction [22]–[24] and adhesion recovery phenomena [25]–[27] as well as curve lubrication are neglected.

2.2 Wear computation

The worn wheel profile is computed using the Archard wear law in both global and local forms. The global computation of wear is performed using the Simpack wear module, while the local computation is carried out by means of a dedicated Matlab routine, which reads the contact patch data obtained from the dynamic simulation.

The Simpack wear module computes the worn volume ΔW in each contact point position for each time step according to eqn (1), in which N is the normal load, H is the hardness of the softer material, s is the total sliding distance and k_{Arch} is the wear coefficient, which is a function of sliding speed and contact pressure. The wear coefficient is obtained from the KTH wear map as a function of the contact pressure and of the sliding speed, with a reduction of the nominal values by a factor 7 to account for natural contamination at the wheel–rail contact, as suggested by Jendel [28] and Jendel and Berg [29]. Fig. 3 shows the Archard wear map and the wear coefficients adopted in the present work. The hardness of the wheel and rail steels is assumed to be equal to 300 HB.

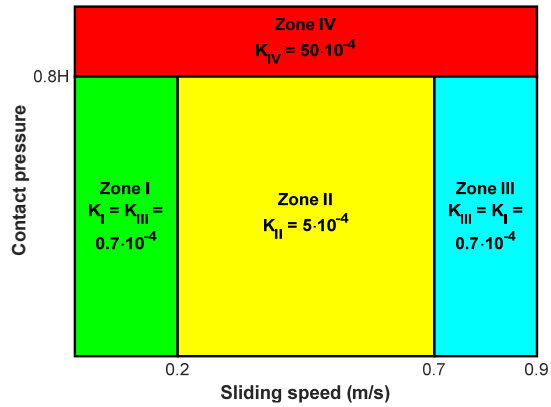

Figure 3: Archard map adopted in the present work.

When the Archard law is applied globally in the form of eqn (1), a distribution of the normal wear depth along the contact patch lateral coordinate must be assumed a priori. The algorithm implemented in the Simpack wear module is transparent for the user, as it is intellectual property of the software house. However, from the total worn volume, Simpack calculates the removed area in a radial section of the wheel ΔA with eqn (2), in which R_{cp} is the wheel radius at the contact point position. Finally, the normal worn depth Δz_n in each lateral position of the contact patch y is calculated introducing an a priori distribution, which unfortunately is not specified by the software developers. In the present work, a global wear algorithm was developed and implemented in a dedicated Matlab routine to compare its results with the outputs of the Simpack wear module. The normal wear depth distribution considered in the in-house Matlab algorithm is semi-elliptic, see eqn (3), in which b is the lateral semi-axis of the contact ellipse and δ is the contact angle.

$$\Delta W = k_{Arch}\frac{Ns}{H}, \tag{1}$$

$$\Delta A = \frac{\Delta W}{2\pi R_{cp}}, \tag{2}$$

$$\Delta z_n(y) = \frac{2}{\pi}\frac{\Delta A}{b\cos\delta}\sqrt{1-\left({}^{y}/_{b}\right)^2}. \tag{3}$$

To avoid the introduction of an a priori distribution of the wear depth along the contact patch and to increase the numerical accuracy, the Archard wear law can be applied locally in the form of eqn (4) to directly compute the normal wear depth Δz_n in each point of the contact patch, identified by the local coordinate set (x,y), as a function of the normal contact pressure p_z and of the sliding distance s_{el} of an element in the contact patch grid. Please note that the local form of Archard law expressed by eqn (4) is derived from eqn (1) by dividing the left-hand and right-hand sides by the area of an element in the contact patch grid. The sliding distance and sliding speed in each element of the contact patch are computed from by means of a dedicated Matlab function implementing the FASTSIM algorithm.

$$\Delta z_n(x,y) = k_{Arch}\frac{p_z(x,y)s_{el}(x,y)}{H}. \tag{4}$$

To obtain a uniform wheel worn profile, the normal depth distribution is summed along each longitudinal strip and then spread along the circumferential direction, see eqn (5), in which Σ_x represents the summation along the longitudinal strip, V_{ref} is the wheel translational speed and finally Δt is the sampling time of the output results.

$$\Delta z_n(y) = \frac{\sum_x \Delta z_n(x,y)}{2\pi R_{cp}} \cdot V_{ref}\Delta t. \tag{5}$$

Once the distribution of the normal wear depth along the lateral coordinate of the wheel profile is obtained, either with the local or global approach, the wear depths along the lateral and vertical directions ΔY and ΔZ can be calculated according to eqns (6) and (7), in which γ is the local profile gradient. Finally, the worn profile can be obtained by applying the worn depths to the proper profile lateral coordinates, and the vertical wear depth can be interpolated with respect to the original array storing the profile lateral coordinate. The vertical wear depth can then be multiplied by a wear multiplier or distance factor, which magnifies the amount of worn material to speed up the simulation time.

$$\Delta Y = \Delta z_n \frac{1}{\sqrt{1+\gamma^2}}, \tag{6}$$

$$\Delta Z = \Delta z_n \frac{\gamma}{\sqrt{1+\gamma^2}}. \tag{7}$$

3 RESULTS

The current section presents the results of the investigation on the effects of local and global approaches in the computation of the wheel worn profiles. The dynamic simulation was run considering the vehicle and track described in the previous section, and the computation of the worn profile was carried out using both the Simpack wear module, implementing a global algorithm, and the dedicated Matlab routine for the direct computation of the worn depth in each cell of the contact patch. Furthermore, an additional computation of the worn profile was carried out with the in-house Matlab global wear model, relying on a semi-elliptic distribution of the normal wear depth along the contact patch lateral direction. The in-house global model was developed as an alternative to the Simpack wear module with the aim to be used in future works in which the worn profile is fed back to the dynamic simulation, in order to improve the numerical stability of the computation, using a strategy similar to the one described by Bosso and Zampieri [2].

The wear depth computed from the dynamic simulation was magnified introducing a wear multiplier equal to 20, as if the wear computed on the simulated track, with a length of 3.77 km, could be extended to a track with a length of 75.4 km. Obviously, the introduction of wear multipliers can lead to a loss of accuracy of the method and to numerical instabilities, because wear is always assigned to the same positions on the wheel profile. Nonetheless, as the goal of the present work is the comparison between global and local approaches in the same scenario, the wear multiplier is just adopted as a mean to increase the wear depth.

Fig. 4 shows the results of the wear computation performed with the three models, namely the Simpack global module, the in-house Matlab global model and the in-house Matlab local model, while Table 2 presents the worn volume computed by the three methods. Please note that the Simpack wear module does not provide the value of the total worn volume as an output, while the local algorithm directly provides the wear depth rather than the removed volume. Nonetheless, the worn volume can be estimated from the Z coordinates of the original (Z_{or}) and worn (Z_{worn}) profiles according to eqn (8), in which Y_s and Y_f are the limit coordinates of the wheel profile and R_w is the wheel radius evaluated in each lateral position Y.

$$\Delta W = \int_{Y_s}^{Y_f} [Z_{or}(Y) - Z_{worn}(Y)] \cdot 2\pi R_w(Y) dY. \tag{8}$$

As noticeable from Fig. 4(a), all three models compute the maximum wear depth in the zone near the flange, where large creepage values arise during curve negotiation. Fig. 4(b) shows a zoomed view in the flange zone, while Fig. 4(c) presents a zoom in the tread zone. The local model is the one that computes the largest peak in the flange zone, while in the tread zone, the global approaches calculate higher values of wear depth, and this explains why the local model is the one that computes the lowest worn volume. The explanation to this behaviour can be given by observing the wear regime calculated in each element of the contact patch grid for a contact position in the flange zone, see Fig. 5(a), and for a contact position in the tread zone, see Fig. 5(b).

The wear regime computed for both cases by the global wear model corresponds to zone I of the KTH wear map, see Fig. 3. As shown in Fig. 5(a), in the flange contact point, one element in the contact patch falls in the catastrophic regime. As the coefficient for the catastrophic regime is 10 times higher with respect to the coefficient of the mild zone, a local generation of catastrophic wear can indeed lead to a wear peak. On the other hand, in the tread contact, see Fig. 5(b), a large portion of the contact patch is in full adhesion conditions, and wear zone I is detected for a small number of elements, while the global wear model

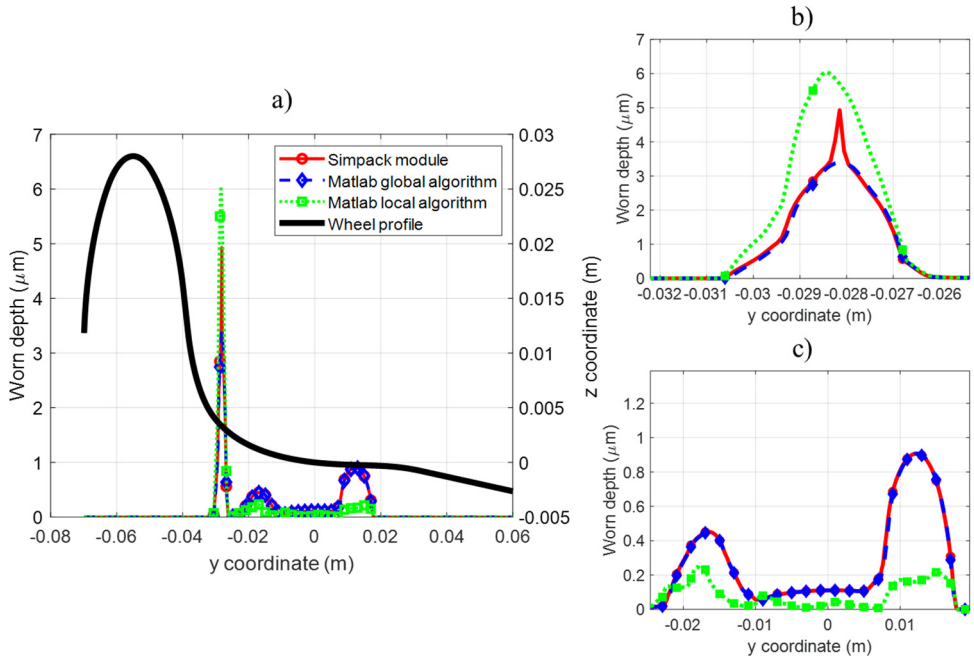

Figure 4: Results of the wear computation. (a) Wear depth along the lateral coordinate; (b) Zoomed view in the flange zone; and (c) Zoomed view in the tread zone.

Table 2: Worn volume computed by the three algorithms.

Model	Worn volume (mm^3)
Simpack wear module	57.9
Matlab global model	56.3
Matlab local model	47.0

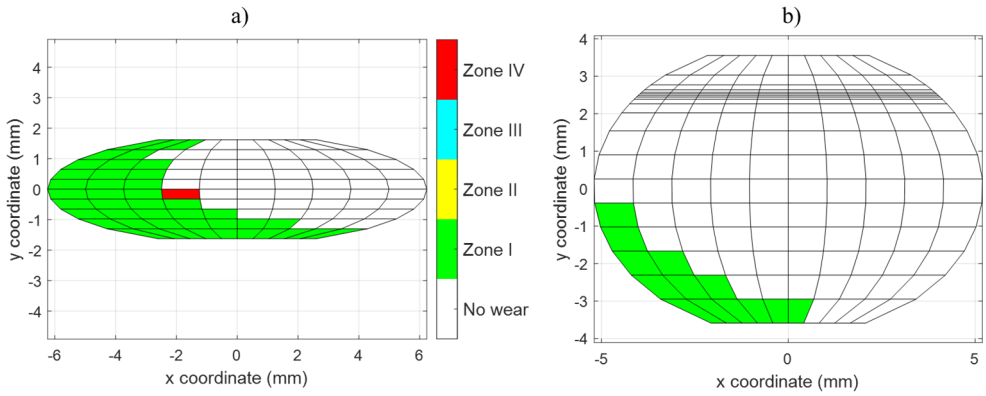

Figure 5: Wear regime computed in the contact patch. (a) Contact near the flange; and (b) Contact in the tread zone.

considers a wear loss on the whole patch. Therefore, the wear depth computed with the local approach is lower with respect to the wear depth computed with the global model for a contact position in the tread zone. Please note that another source of discrepancy between the global and local approaches is the assumption of the distribution of the traction bound. In the global approach, the Hertzian pressure is used to determine the wear regime, while in the local approach, a parabolic distribution is assumed. The parabolic distribution is preferred over the elliptic one as it gives a more accurate division between the adhesion and slip zone in the contact patch when using the FASTSIM algorithm [30].

Focusing again on Fig. 4, the global model developed by the authors is in excellent agreement with the wear depth provided by Simpack in the tread zone, while in the flange zone the Matlab global algorithm misses the wear peak computed by the Simpack algorithm at the lateral position of −0.028 m. This discrepancy can be mainly related (but not limited) to the two possible reasons listed below:

1. The a priori distribution of the wear depth adopted by the Simpack wear module is not known and it may differ from the semi-elliptic distribution implemented in the in-house Matlab wear module, especially in case the Simpack module considers the penetration distribution and the real shape of the contact patch.
2. The Matlab global wear routine uses interpolation strategies that may differ with respect to the ones adopted by the Simpack algorithm.

Finally, for what concerns the computational times, several runs were launched with both the Matlab global and local algorithms, as the code is not run in real-time, and the global method proved to ensure a speedup by a factor equal to 1.58. Obviously, the global method is faster because it saves the time required to discretize the contact patch.

4 CONCLUSIONS

The main outcomes of the numerical activity presented in the previous sections are summarized in the following bulleted list.

- The application of the Archard wear law in the global form overestimates wear in the tread zone, while slightly underestimating wear in the flange.
- The generation of catastrophic wear in even a small number of elements in the contact patch grid can lead to high wear peaks, because the wear coefficient in the catastrophic regime is ten times higher compared to the wear coefficient in the mild regime.
- In the tread zone, the global approach calculates wear on the whole extension of the contact patch, but a local analysis shows that typically only a small number of elements produces wear, as most of the contact patch is in full adhesion.
- The global method developed by the authors provides results in good agreement with the outputs of the Simpack wear module, although in the flange zone a wear peak is missed, probably due to differences in the interpolation strategies and in the wear depth distributions.
- The global approach speeds up the computation by a factor equal to approximately 1.58 compared to the local method. As the local approach is clearly more accurate, because it distinguishes between slip and adhesion zones in the contact patch and it directly computes the wear depth, the local approach is the better choice when the goal of the simulation is a detailed prediction of the wheel life. On the other hand, if the computation only aims at assessing the influence of several parameters on wear, the global method can be a reliable solution to ensure fast simulation times.

To gain a better understanding of the problem, further investigations, should be carried out, see the bulleted list below.

- The numerical activity performed in the context of the present work should be extended to consider different types of vehicles and different track layouts.
- The comparison between local and global approaches should be extended to the Krause–Poll law, which is the energy-based wear law available in Simpack. To the authors' knowledge, the adoption of the Krause–Poll law in local form is currently not witnessed in the literature, but the authors recognize that this wear equation can be easily written in local form if the dissipated energy is computed locally in each cell of the contact patch grid.
- Numerical simulations relying on a loop of dynamic simulations with worn profiles should be performed, to investigate how the differences between local and global approaches increase during the simulation.

REFERENCES

[1] Bosso, N., Magelli, M. & Zampieri, N., Simulation of wheel and rail profile wear: A Review of numerical models. *Railway Engineering Science*, in print.

[2] Bosso, N. & Zampieri, N., Numerical stability of co-simulation approaches to evaluate wheel profile evolution due to wear. *International Journal of Rail Transportation,* **8**(2), pp. 159–179, 2020. DOI: 10.1080/23248378.2019.1672588.

[3] Abeidi, A.S., Bosso, N., Gugliotta, A. & Somà, A., Numerical simulation of wear in railway wheel profiles. *Proceedings of the 8th Biennial ASME Conference on Engineering Systems Design and Analysis, ESDA2006*, pp. 963–977, 2006. DOI: 10.1115/ESDA2006-95571.

[4] Bosso, N., Gugliotta, A. & Abeidi, A.S., Influence of vehicle dynamics on wear of railway wheel profiles. *International Journal of Applied Engineering Research,* **13**(6), pp. 3540–3549, 2018.

[5] Archard, J.F., Contact and rubbing of flat surfaces. *Journal of Applied Physics,* **24**(8), pp. 981–988, 1953. DOI: 10.1063/1.1721448.

[6] Archard, J.F., Hirst, W. & Allibone, T.E., The wear of metals under unlubricated conditions. *Proceedings of the Royal Society of London Series A: Mathematical and Physical Sciences*, **236**(1206), pp. 397–410, 1956. DOI: 10.1098/rspa.1956.0144.

[7] McEwen, I.J. & Harvey, R.F., Interpretation of wheel/rail wear numbers. Railway Technical Centre, Report No. TM VDY 004, 1986.

[8] Lewis, R. et al., Integrating dynamics and wear modelling to predict railway wheel profile evolution. Presented at the *6th International Conference on Contact Mechanics and Wear of Rail/Wheel Systems: CM2003*, Gothenburg, Sweden, 2003.

[9] Krause, H. & Poll, G., Wear of wheel–rail surfaces. *Wear,* **113**(1), pp. 103–122, 1986. DOI: 10.1016/0043-1648(86)90060-8.

[10] Zobory, I., Prediction of wheel/rail profile wear. *Vehicle System Dynamics,* **28**(2–3), pp. 221–259, 1997. DOI: 10.1080/00423119708969355.

[11] Peng, B., Iwnicki, S., Shackleton, P. & Crosbee, D., Comparison of wear models for simulation of railway wheel polygonization. *Wear,* **436**–**437**, 2019. DOI: 10.1016/j.wear.2019.203010.

[12] Lewis, R., Kuka, N., Ariaudo, C., Dwyer-Joyce, R., Tassini, N. & Quost, X., Predicting railway wheel wear starting from multi-body analysis: A preliminary study. Presented at the *IEEE/ASME/ASCE 2008 Joint Rail Conference*, Wilmington, DE, 2008. DOI: 10.1115/JRC2008-63021.

[13] Ignesti, M., Innocenti, A., Marini, L., Meli, E. & Rindi, A., Development of a model for the simultaneous analysis of wheel and rail wear in railway systems. *Multibody System Dynamics,* **31**(2), pp. 191–240, 2014. DOI: 10.1007/s11044-013-9360-0.
[14] Shen, Z.Y., Hedrick, J.K. & Elkins, J.A., A comparison of alternative creep force models for rail vehicle dynamic analysis. *Vehicle System Dynamics,* **12**(1–3), pp. 79–83, 1983. DOI: 10.1080/00423118308968725.
[15] Polach, O., A fast wheel–rail forces calculation computer code. *Vehicle System Dynamics,* **33**(sup1), pp. 728–739, 1999. DOI: 10.1080/00423114.1999.12063125.
[16] Bosso, N. & Zampieri, N., A novel analytical method to calculate wheel–rail tangential forces and validation on a scaled roller-rig. *Advances in Tribology,* **2018**, 2018. DOI: 10.1155/2018/7298236.
[17] Enblom, R. & Berg, M., Impact of non-elliptic contact modelling in wheel wear simulation. *Wear,* **265**(9), pp. 1532–1541, 2008. DOI: 10.1016/j.wear.2008.01.027.
[18] Kaiser, I., Poll, G. & Vinolas, J., Modelling the impact of structural flexibility of wheelsets and rails on the wheel–rail contact and the wear. *Wear*, 2020. DOI: 10.1016/j.wear.2020.203445.
[19] Kalker, J.J., A fast algorithm for the simplified theory of rolling contact. *Vehicle System Dynamics,* **11**(1), pp. 1–13, 1982. DOI: 10.1080/00423118208968684.
[20] Vollebregt, E.A.H., Use of "CONTACT" in multi-body vehicle dynamics and profile wear simulation: initial results. *Proceedings of the 22nd International Symposium on Dynamics of Vehicles on Roads and Tracks*, 2013.
[21] Piotrowski, J. & Kik, W., A simplified model of wheel/rail contact mechanics for non-Hertzian problems and its application in rail vehicle dynamic simulations. *Vehicle System Dynamics,* **46**(1–2), pp. 27–48, 2008. DOI: 10.1080/00423110701586444.
[22] Monk-Steel, A.D., Thompson, D.J., de Beer, F.G. & Janssens, M.H.A., An investigation into the influence of longitudinal creepage on railway squeal noise due to lateral creepage. *Journal of Sound and Vibration,* **293**(3), pp. 766–776, 2006. DOI: 10.1016/j.jsv.2005.12.004.
[23] Spiryagin, M., Polach, O. & Cole, C., Creep force modelling for rail traction vehicles based on the Fastsim algorithm. *Vehicle System Dynamics,* **51**(11), pp. 1765–1783, 2013. DOI: 10.1080/00423114.2013.826370.
[24] Vollebregt, E.A.H., Numerical modeling of measured railway creep versus creep-force curves with CONTACT. *Wear,* **314**(1), pp. 87–95, 2014. DOI: 10.1016/j.wear.2013.11.030.
[25] Bosso, N., Gugliotta, A., Magelli, M., Oresta, I.F. & Zampieri, N., Study of wheel–rail adhesion during braking maneuvers. *Procedia Structural Integrity,* **24**, pp. 680–691, 2019. DOI: 10.1016/j.prostr.2020.02.060.
[26] Bosso, N., Gugliotta, A., Magelli, M. & Zampieri, N., Experimental setup of an innovative multi-axle roller rig for the investigation of the adhesion recovery phenomenon. *Experimental Techniques,* **43**(6), pp. 695–706, 2019. DOI: 10.1007/s40799-019-00327-x.
[27] Bosso, N., Magelli, M. & Zampieri, N., Investigation of adhesion recovery phenomenon using a scaled roller-rig. *Vehicle System Dynamics,* **59**(2), pp. 295–312, 2021. DOI: 10.1080/00423114.2019.1677922.
[28] Jendel, T., Prediction of wheel profile wear: Comparisons with field measurements. *Wear,* **253**(1), pp. 89–99, 2002. DOI: 10.1016/S0043-1648(02)00087-X.
[29] Jendel, T. & Berg, M., Prediction of wheel profile wear. *Vehicle System Dynamics,* **37**(sup1), pp. 502–513, 2002. DOI: 10.1080/00423114.2002.11666258.

[30] Vollebregt, E.A.H. & Wilders, P., FASTSIM2: A second-order accurate frictional rolling contact algorithm. *Computational Mechanics,* **47**(1), pp. 105–116, 2011. DOI: 10.1007/s00466-010-0536-7.